NUMERICAL EVALUATION OF GOLDEN RULE RATES FOR CONDENSED PHASE PROCESSES

Eyal Neria and Abraham Nitzan
School of Chemistry, the Sackler Faculty of Science
Tel Aviv University, Tel Aviv, 69978, Israel

Abstract

Our recently proposed method for the numerical evaluation of golden rule rates of non-adiabatic transitions in condensed phases is generalized. As before, the method is based on propagating Gaussian wavepackets on the initial and final electronic potential surfaces. In the present paper these Gaussians are thermal wavefunctions obtained by thermal propagation of eigenfunction of the position operator using either the high temperature limit of the propagator or the local harmonic approximation to it. The high T limit is essentially equivalent to our previously suggested procedure, but is more rigorously defined. The local harmonic approximation makes it possible to extend the method to low temperature situations. The performance of the method relative to other available procedures is examined by model calculations.

I. Introduction

Numerical simulations of quantum processes in condensed phases are rapidly becoming a major tool in studies of quantum dynamical phenomena in such environments.[1-4] The complexity of the system requires a mixed quantum-classical description of the system, since a full quantum description is expected to remain beyond computer capabilities in the foreseeable future. A particularly challenging problem arises in processes involving two or more electronic states, *e.g.* processes involving non-adiabatic transitions in solutions.[5-18] The difficulty originates from the fact that the solvent responds differently to different solute electronic states, implying that a fully classical description of the solvent may not be sufficient.[4] The difficulties involved were nicely summarized by Tully.[5] Recently used methods are: (a) Generalizations of the surface hopping (Tully-Preston)[6] procedure to condensed phase environments. (b) Multiconfiguration time dependent self consistent field (MCTDSCF) approximations.[8] (c) Application of the Pechukas theory[9] for non-adiabatic processes in mixed quantum-classical systems.[10] (d) Tully's molecular dynamics with electronic transitions (MDET) algorithm.[5,11] (e) Simulations of non-adiabatic transition rates based on the golden rule (GR) or its generalizations.[12-19]

In recent publications[13] we have proposed a semiclassical method for calculating thermal non adiabatic transition rates involving a quantum subsystem interacting with an otherwise essentially classical solvent. Although the solvent interacts differently with the solute in different quantum states, only classical information on its motion is required. The method is based on the correlation time representation of the golden rule formula for the transition rate between two electronic states, $|1\rangle$ and $|2\rangle$,

$$k_{1\to 2} = \int_{-\infty}^{\infty} dt\, e^{i\Delta E t/\hbar} C(t) \qquad (1)$$

where $\Delta E = E_2 - E_1$ is the difference between the energy origin of surfaces 1 and 2 and where

$$C(t) = Z_1^{-1}\hbar^{-2}\sum_i e^{-\beta E_i}\langle i|F_{21}|i\rangle \equiv \hbar^{-2}\langle F_{21}\rangle_T \qquad (2)$$

and

$$F_{21} = V_{12}e^{iH_2 t/\hbar}V_{21}e^{-iH_1 t/\hbar} \qquad (3)$$

In equations (2) and (3) $|i\rangle$ are the nuclear states associated with the initial electronic surface,

$\beta = (k_B T)^{-1}$ and $Z_1 = \sum_i e^{-\beta E_i}$ where the sum is over all vibronic levels belonging to $|1\rangle$. H_1 and H_2 are the nuclear Hamiltonians associated with the electronic states $|1\rangle$ and $|2\rangle$ respectively, each measured from its own electronic origin, and V is the operator responsible for the transition between the two electronic states. $V_{12} = \langle 1|V|2\rangle$ is an operator in the space of the nuclear degrees of freedom. In our previous work[13a,b] we have evaluated C(t) by representing the nuclear wavefunction by a product of Gaussian wavepackets with fixed width and with average positions and momenta sampled from a canonic (classical or quantum; *i.e.* Wigner) distribution. An initial wavepacket which is taken to be a product of one dimensional wavepackets

$$G(\mathbf{x}, t=0) = \left(\frac{a}{\pi}\right)^{1/4} \times \exp\left[\tfrac{1}{2}a(\mathbf{x}-\mathbf{x}_0)^2 + i\mathbf{p}\cdot(\mathbf{x}-\mathbf{x}_0)\right] \quad (4)$$

is propagated using the frozen Gaussians approximation (FGA),[20] as outlined in Appendix A. The propagation of the wavepacket is determined by the classical trajectory with initial positions $\mathbf{x}_0$ and momenta $\mathbf{p}_0$. C(t) is then essentially the overlap integral at time t between the wavepackets obtained by propagating G(x,t=0) on each potential surface. The nuclear operators V_{12} and V_{21} in (3) are replaced by their classical analogs, evaluated at the centers of the initial wavepacket G(x,t=0) and the wavepacket $e^{-iH_1 t/\hbar}|G(\mathbf{x}, t=0)\rangle$ respectively. The rational beyond using the crude FGA propagation method is that C(t) decays quickly, and during its short lifetime quantum effects such as the spreading of the wave functions may be disregarded. In this case the only evolution of importance is associated with the underlying classical evolution of the packet center. A drawback of this approach is the appearance of the widths of the gaussian wavepackets, $a^{-1/2}$, as undetermined parameters of this procedure. These widths were chosen to minimize the resulting error in C(t) when compared to the exact result for the analytically soluble model of displaced harmonic oscillators. In the high temperature limit the resulting width is proportional to the thermal de Broglie wavelength $\lambda_{th} = [2\pi/(mk_B T)]^{1/2}\hbar$, $a^{-1/2} \cong 1/6\lambda_{th}$. Furthermore, the result for the rate (at high T) is not very sensitive to this choice, within two orders of magnitudes of the prescribed value.

Other methods for simulating GR rates were described in the literature.[14-19] In particular Warshel,[17] Mukamel[18] and Hynes[19] and co-workers have rewritten Eqs. (2) and (3), with V_{12} taken constant for simplicity, in the form[12]

$$C(t) = \frac{|V_{12}|^2}{\hbar^2}\left\langle \exp_-\left\{\frac{i}{\hbar}\int_0^t d\tau U_1(\tau)\right\}\right\rangle \quad (5)$$

where $U=H_2-H_1$ is the difference between the nuclear potential surfaces in the final and initial electronic states,

$$U_1(\tau) = e^{iH_1\tau}Ue^{-iH_1\tau} \quad (6)$$

and where the subscript (-) on the exponential function denoted negative time ordering (later times on the right). $\langle\ \rangle_T$ denotes thermal average associated with nuclear equilibrium in the initial electronic state. A semiclassical approximation can be made at this point by replacing $U_1(t)$ by its classical analog, $U_1(t) = U^c(x^1(t))$, where $x^1(t)$ stands for the position associated with classical trajectories evaluated on the initial electronic surface. The thermal average is then performed by using a thermal distribution of the initial conditions for these trajectories. obviously the time ordering in Eq. (5) is irrelevant in this approximation.

A direct use of Eq. (5) may be difficult in actual applications because the exponent in the equation is a rapidly oscillating function of absolute magnitude equal to 1, and the decay of C(t) in time is obtained from destructive interference of such terms. A useful approximation[12,17-19] is obtained by performing a cumulant expansion up to second order, yielding

$$C(t) = \frac{|V_{12}|^2}{\hbar^2} \times \exp\left\{-i/\hbar M^{(1)}(t) - 1/\hbar^2 M^{(2)}(t)\right\} \quad (7)$$

with $M^{(1)}(t)$ and $M^{(2)}(t)$ given by

$$M^{(1)}(t) = \int_0^t dt' \langle U(t') \rangle \qquad (8a)$$

and

$$M^{(2)}(t) = \int_0^t dt' \int_0^{t'} dt'' \left[\langle U(t'')U(t') \rangle - \langle U(t'') \rangle \langle U(t') \rangle \right] \qquad (8b)$$

The time ordering implied in Eq. (5) is carried over to Eq. (8b), however if U (t) is replaced by $U^c\left(x^1(t)\right)$ as before, this ordering becomes irrelevant.

A consistency check on this approximation may be obtained by noting that an alternative form of Eq. (5) is given by

$$C(t) = \frac{|V_{12}|^2}{\hbar^2} \left\langle \exp_+ \left\{ \frac{i}{\hbar} \int_0^t d\tau U_2(\tau) \right\} \right\rangle \qquad (9)$$

where $U_2(t) = e^{iH_2 t} U e^{-iH_2 t}$ and where the subscript (+) denotes positive time ordering. In the semiclassical approximation $U_2(t)$ is replaced by $U^c\left(x^2(t)\right)$ where the trajectories are now evaluated on the final potential surface. In the semiclassical and second order cumulant approximations Eq. (9) leads to equations identical to Eqs. (7)-(8) with $U_1(t)$ replaced by $U_2(t)$. *Note however that the average over initial condition is associated with a thermal distribution on the initial electronic state as before.* An agreement between the results obtained from these alternative procedures (that should yield identical results if no approximations are made) is a consistency check for the accuracy of the method.

In the present paper we describe two modified versions of our golden rule (GR) simulation procedure. These new formulations become exact in the high temperature limit and one of them is potentially applicable also at low temperatures. Both eliminate the need for approximate prescriptions for the initial widths of the Gaussian wavepackets. In the FGA these widths are kept constant, but 'thawed' Gaussians with time varying widths[21] can be used with almost the same computational effort. We examine the performance of these methods by comparing them to exact calculations with simple models. We also compare the results to those obtained using our previous procedure,[13b] as well as to calculations based on the classical analog of (5) and on the approximations (7)-(8).

II. Calculation with thermal wavepackets

The correlation function C(t), Eq. (2), can be written as a trace in the position space representation

$$C(t) = \frac{1}{Z_1 \hbar^2} \int dx' \langle x' | e^{-\frac{1}{2}\beta H_1} F_{21} e^{-\frac{1}{2}\beta H_1} | x' \rangle = \frac{1}{Z_1 \hbar^2} \int dx' \, e^{-\beta V_1(x')} \langle \Psi_{x'} | F_{21} | \Psi_{x'} \rangle \qquad (10)$$

where

$$\Psi_{x'} = \exp\left[-\tfrac{1}{2}\beta\left(H_1 - V_1(x')\right)\right] | x' \rangle \qquad (11)$$

To continue with our method as outlined above we need to express $\Psi_{x'}$ as a Gaussian. We follow Hellsing et al[22] who have used such *thermal wavepackets* obtained from either the high temperature limit (HTL) or from the local harmonic approximation (LHA).

In the high temperature limit j , Eq. (11), can be approximated by

$$\Psi_{x'}(x) = \exp\left[-\tfrac{1}{2}\beta\left(H_1(x) - V_1(x')\right)\right]\delta(x - x') = \left[\frac{m^3}{\pi^3 \hbar^6 \beta^3}\right]^{d/2} g_{x'}(x) \qquad (12)$$

where x is the position in the (d dimensional) configuration space and

$$g_{x'}(x) = \left[\frac{2mk_B T}{\pi\hbar^2}\right]^{d/4} \exp\left\{-\frac{mk_B T}{\hbar^2}(x - x')^2\right\} \qquad (13)$$

Also in this limit

$$Z_1 = \left[\frac{m}{\pi\hbar^2\beta}\right]^{d/3} Q_1 \qquad (14)$$

where

$$Q_1 = \int dx \, e^{-\beta V_1(x)} \qquad (15)$$

Eqs (12)-(14) are obtained by using, for $\beta\to 0$, $\exp[-\beta(T+V_1)]=\exp(-\beta T)\exp(-\beta V_1)+O(\beta^2)$. Eqs. (10), (12)-(14) lead to

$$C(t)=\frac{1}{Q_1\hbar^2}\int d\mathbf{x}'\, e^{-\beta V_1(\mathbf{x}')} \times\left\langle g_{\mathbf{x}'}\left|V_{12}e^{iH_2t/\hbar}V_{21}e^{-iH_1t/\hbar}\right|g_{\mathbf{x}'}\right\rangle \quad (16)$$

Thus, in this limit, the numerical evaluation of C(t) proceeds as described in Sect. I (and in Refs. 13), except that the functions (13) are zero momentum wavepackets. The centers of these initial wavepackets are sampled from a Boltzmann distribution in configuration space, as shown in Eq. (16), not in phase space, implying considerable saving in computing effort. The width of the Gaussian is essentially the thermal de Broglie wavelength, as anticipated in our earlier procedure.[13]

Another way to express $\Psi_{x'}$ by a Gaussian is provided by the local harmonic approximation (LHA). For simplicity we limit our discussion to the one dimensional case. The multidimensional problem is considered in Appendix B.

The LHA is obtained by expanding the potential $V_1(x)$ up to quadratic terms about the point of interest (x' in Eq. (11)),

$$V_1(x)\ -\ V_1(x')=\eta(x')(x-x')+\tfrac{1}{2}k(x')(x-x')^2 \quad (17)$$

where $\eta=\partial V_1/\partial x$ and $k=\partial^2 V_1/\partial x^2$. Using this approximation in Eq. (11) leads to

$$\Psi_{x'}(x)=\exp\left[-\tfrac{1}{2}\beta(H_1(x)-V_1(x'))\right]\ \delta(x-x') \cong\exp\left\{\frac{\beta\eta^2}{4k}\right\}G_{har}\left(x-x'-\frac{\eta}{k},\frac{\eta}{k};-i\hbar\beta/2\right) \quad (18)$$

where G_{har} is the harmonic oscillator Green's function given by

$$G_{har}(x_a,x_b;t)=\left(\frac{m\omega}{2\pi i\hbar\sin(\omega t)}\right)\exp\left\{\frac{im\omega}{2\hbar\sin(\omega t)}\times\left[\left(x_b^2+x_a^2\right)\cos(\omega t)-2x_ax_b\right]\right\} \quad (19)$$

with h, k and $\omega=\sqrt{k/m}$ evaluated at the point x'. The appearance of the position dependent frequency $\omega(x')$ underlines the local nature of this approximation. Eq. (18) may be rewritten in the form of a Gaussian wavepacket centered about a shifted position x_m:

$$\Psi_{x'}(x)=\left(\frac{m\omega}{2\pi\hbar\sinh(\beta\hbar\omega)}\right)^{1/4}\exp\left\{\frac{\beta\eta^2}{4k}-\frac{m\omega}{2\hbar}\left(\frac{\eta}{k}\right)^2\tanh\left(\tfrac{1}{2}\beta\hbar\omega\right)\right\}g_{x_m} \quad (20)$$

with g_{x_m} given by

$$g_{x_m}(x)=\left(\frac{m\omega\coth(\beta\hbar\omega)}{\pi\hbar}\right)^{1/4}\times\exp\left\{\frac{m\omega}{2\hbar}\coth\left(\tfrac{1}{2}\beta\hbar\omega\right)(x-x_m)^2\right\} \quad (21)$$

and with

$$x_m(x')=x'-\frac{\eta}{k}\left[1-\sec h\left(\tfrac{1}{2}\beta\hbar\omega\right)\right] \quad (22)$$

It should be kept in mind that in equations (18)-(22) $\omega=\omega(x')$, $\eta=\eta(x')$ and $k=k(x')$. Inserting Eqs. (20)-(22) in Eq. (10) leads to

$$C(t)=\frac{1}{Z_1\hbar^2}\int dx'\,P(x') \times\left\langle g_{x_m}\left|V_{12}e^{iH_2t/\hbar}V_{21}e^{-iH_1t/\hbar}\right|g_{x_m}\right\rangle \quad (23a)$$

where

$$P(x)=\left\{\frac{m\omega(x)}{2\pi\hbar\sinh(\beta\hbar\omega(x)}\right\}^{1/2}$$
$$\times\exp\left\{\frac{\beta\eta^2(x)}{2k(x)}-\beta V_1(x)\right.$$
$$\left.-\frac{m\omega(x)}{\hbar}\left[\frac{\eta(x)}{k(x)}\right]^2\tanh(1/2\beta\hbar\omega(x))\right\} \quad (23b)$$

and

$$Z_1=\int dx\,P(x) \quad (23c)$$

This result provides a new prescription for evaluating C(t) within the LHA: A configuration x' is sampled from the (unnormalized) probability function P(x') which is a modification of the usual canonic distribution. This can be done using a Monte Carlo sampling procedure. The point x' is then shifted to x_m according to Eq. (22) and a Gaussian wavepacket g_{x_m} of the form (21) is located, centered at this point. This Gaussian is propagated with the FGA as before, leading to the expectation value in (23); the integral over x' is the average obtained from this sampling procedure. The following points should be noted:

(a). The Gaussian width is now a function of x, given by

$$a(x)^{-1/2}=\left\{\frac{\hbar}{m\omega(x)\coth\left(\frac{1}{2}\beta\hbar\omega(x)\right)}\right\}^{1/2} \quad (24)$$

In the high temperature limit, $\hbar\omega(x)<<k_BT$, this becomes $a^{-1/2}=\hbar(2mk_BT)^{-1/2}$ which is position independent and leads to the high temperature result given above, Eq. (13). In fact, it is straightforward to show that in this limit Eqs. (13), (15)-(16) are recovered.

(b) As before, and in contrast to our original procedure, the sampling is performed in configuration space, not in phase space, implying considerable saving of computing effort.

(c) If the initial surface is harmonic, $V_1=\frac{1}{2}m\omega^2x^2$, Eq. (23) is exact (within the GR formalism). In this case the correlation function has the simpler form

$$C(t)=\frac{1}{Z_1\hbar^2}\int dx'\,P(x')$$
$$\times\left\langle g_{x_m}\left|V_{12}e^{iH_2t/\hbar}V_{21}e^{-iH_1t/\hbar}\right|g_{x_m}\right\rangle \quad (25a)$$

with $x_m=x'/\cosh(1/2\beta\hbar\omega)$,

$$P(x)=\left\{\frac{m\omega}{2\pi\hbar\sinh(\beta\hbar\omega)}\right\}^{1/2}$$
$$\times\exp\left\{-\frac{m\omega}{\hbar}\tanh(\tfrac{1}{2}\beta\hbar\omega)x^2\right\} \quad (25b)$$

and

$$Z_1=\int dx\,P(x)=\left\{\frac{m\omega}{2\pi\hbar\sinh(\beta\hbar\omega)}\right\}^{1/2}$$
$$\times\left\{\frac{\pi\hbar}{m\omega\tanh(\beta\hbar\omega/2)}\right\} \quad (25c)$$

The distribution P(x) is essentially the thermal Wigner function[23] of the harmonic oscillator integrated over the momentum.

(d). The weight functions P(x), Eqs. (23b) and (25b) depend on the local frequency w(x), therefore the execution of this procedure for a general many body potential surface requires additional considerations (see Appendix B). In the high temperature limit the calculation of C(t), Eq. (16), involves the simple Boltzmann weight $e^{-\beta V(x)}$, and simple Monte Carlo procedures can be used.

(e). The harmonic approximation which leads to equations (23) is valid only if k(x')$0. Furthermore, if k(x')<0 an expansion about x' leads to imaginary ω(x') and, while giving a formally valid procedure, may cause large errors associated with the fact that x_m becomes a highly oscillating function of the temperature as T→0. Large errors are also expected in the contributions from positions x' for which |k(x')| is

small so that $|x_m(x')-x'|$ is large (see Eq.(22)). In this case the thermal propagation, Eq. (18), which transform $\delta(x-x')$ to a Gaussian centered at x_m using a Hamiltonian valid only for x close to x', will cause large deviations from the corresponding exact propagation. This can be seen by considering the low temperature limit of Eq.(23b), $P(x) = \exp(-\beta W(x))$ where

$W(x) = V_1(x) - \frac{\eta^2(x)}{2k(x)} - \frac{m\omega(x)}{\hbar\beta}\left(\frac{\eta(x)}{k(x)}\right)^2$. If $V_1(x)$ is harmonic, the first two terms in W(x) vanish and β W(x) becomes the familiar ground state distribution of the quantum harmonic oscillator. In other cases these two terms may dominate the distribution in the $T\to 0$ limit. In particular note that $W(x;T=0) = V_1(x) - \eta^2(x)/2k(x)$ has minima at points that satisfy $\eta(x) \neq 0$, $k'(x)=0$ and $k''(x)>0$, so such points will dominate the distribution $e^{-\beta W(x)}$ as $T \to 0$, a property not shared by the exact thermal distribution.

These difficulties may be overcome in the low T limit by (1) using $e^{-\beta V_1(x)}$ rather than P(x) as the weight function in the sampling used to evaluate the integral (23a); (2) discarding points x' for which $k(x')\leq 0$ from the integrals (23a) and (23c); (3) including points x' with $k(x')>0$ only provided that k(x') is not too small, so that such points are not too close to the singularity of W(x). The last restriction is somewhat vague and its quantitative definition ($\hbar\omega(x')>\beta^{-1}$ seems a reasonable choice) will be considered elsewhere. Note that using $e^{-\beta V_1(x)}$ as weight function focus the integration near the local minima in the potential, while the other two conditions restrict the integration to regions about these minima, eliminating regions of imaginary, zero or inconveniently small frequency. Obviously the suggested procedure keeps the most important x' regions in the low T limit.

(f). In the applications presented below we use the FGA for the propagation of the Gaussian wavepackets. This is often justified, in particular for many body systems, as discussed above. More accurate semiclassical propagation methods, such as the original Heller method may be used if needed.

In the next section we compare the performance of the methods discussed above when applied to simple exactly soluble models.

III Model Calculations

IIIa. Transition between harmonic and linear potential surfaces. A simple exactly soluble model that was considered in our earlier work[13b] consists of two diabatic surfaces: The initial electronic state $|1\rangle$ is associated with a harmonic potential and is coupled to another state $|2\rangle$ characterized by a linear potential (Fig. 1). The coupling V_{12} is assumed constant. The potential surfaces are given, in dimensionless units, by

$$V_1 = \frac{1}{2}X^2 \qquad (26a)$$

$$V_2 = \alpha X + E_0 \qquad (26b)$$

These surfaces cross at energy $V_c = \alpha \pm \sqrt{\alpha^2 + 2E_0}$. Note that propagation with 'thawed' Gaussians[21] (but not with frozen Gaussians) is exact on these surfaces.

Consider first transitions out of a single quantum level $|i\rangle$ of the harmonic surface. The GR rate is given by Eq. (1), where $C(t) = \hbar^{-2}\langle i|F_{21}|i\rangle$ F_{21} is given by Eq. (3). This implies a microcanonical sampling instead of the canonical sampling performed in Eq. (2). The state $|i\rangle$ is then expanded in Gaussians, $|i\rangle = \sum_k C_{ik}|g_k\rangle$ (see Ref. 13b), so that $C(t) = \hbar^{-2}\sum_k\sum_{k'} C_{ik}^* C_{ik'}\langle g_k|F_{21}|g_{k'}\rangle$, and the matrix element $\langle g_k|F_{21}|g_{k'}\rangle$ is calculated using the procedure described in Sect. II. We refer to this as a coherent expansion of C(t), while keeping only diagonal terms leads to an incoherent approximation, $C(t) = \hbar^{-2}\sum_k |C_{ik}|^2\langle g_k|F_{21}|g_k\rangle$, analogous to the thermal rate (16) or (23a). The coherent procedure based on Eq. (1) and the FGA[13b] yield results in very close agreement with the exact rate, and reproduce very well the oscillatory behavior of the rate as a function of V_c (i.e. of E_0) or of the initial quantum level. When incoherent microcanonical sampling is used these oscillations are not reproduced, and an averaged behavior is observed, which suggest (as was confirmed) that incoherent sampling should work well for thermal rates at high enough temperatures.

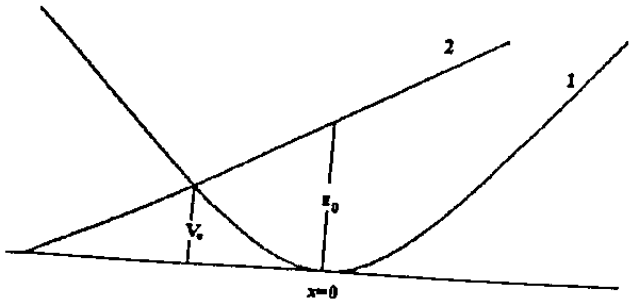

Fig. 1: The potential surfaces in the model defined by Eq. (26).

Of the methods described in Sect II, the high T approximation is essentially equivalent to the procedure used in Ref 13b, while the LHA can potentially improve these results. On the other hand, the methods based on evaluating Eqs. (5)-(6) or (7)-(8) using classical path dynamics on the harmonic potential fail, because U(t) and (consequently) C(t) are obtained in the present model to be oscillatory functions of t, so that the integral (1) does not converge.

Now consider the thermal rates. Again our present formulation of the high T approximation is conceptually more satisfactory then, but technically equivalent to, the method used in our earlier work,[13b] and the LHA method is expected to improve the performance of this approach.

Table I. Thermal transition rates for the model of one dimensional coupled harmonic(initial) and linear (final) surfaces (Eq. 26). α=6 and V =3.5. Shown are the exact golden rule result together with results based on the procedure of Ref 13, on the LHA (Eq. 23), on the HTL (Eqs 13-16), on the classical analog of Eq. (5) with Boltzmann sampling (column LB), Wigner sampling (column LW) and on the cumulant expansion, Eqs (7)-(8) (columns C1 and C2). Columns C1 and C2 give results based on the second order cumulant approximation with the classical dynamics performed on surfaces 1 and 2 respectively.

T	Exact GR	Ref. 12b	LHA	HTL	LB	LW	C1	C2
0.	$7.41\ 10^{-5}$	$7.93\ 10^{-5}$	$7.93\ 10^{-5}$	–	–	$4.24\ 10^{-4}$	–	–
.5	$1.04\ 10^{-3}$	$3.95\ 10^{-4}$	$1.39\ 10^{-3}$	$6.60\ 10^{-3}$	$4.83\ 10^{-4}$	$1.8\ 10^{-3}$	$4.19\ 10^{-5}$	$1.56\ 10^{-3}$
1.	$1.02\ 10^{-2}$	$9.81\ 10^{-3}$	$1.12\ 10^{-2}$	$1.49\ 10^{-2}$	$9.00\ 10^{-3}$	$1.10\ 10^{-2}$	$3.29\ 10^{-3}$	$-4.5\ 10^{-4}$
2.	$3.64\ 10^{-2}$	$3.70\ 10^{-2}$	$3.69\ 10^{-2}$	$3.82\ 10^{-2}$	$3.74\ 10^{-2}$	$3.65\ 10^{-2}$	$2.97\ 10^{-2}$	$2.85\ 10^{-2}$
3.	$5.25\ 10^{-2}$	$5.31\ 10^{-2}$	$5.27\ 10^{-2}$	$5.31\ 10^{-2}$	$5.24\ 10^{-2}$	$5.24\ 10^{-2}$	$5.70\ 10^{-2}$	$5.67\ 10^{-2}$
5.	$6.45\ 10^{-2}$	$6.48\ 10^{-2}$	$6.45\ 10^{-2}$	$6.47\ 10^{-2}$	$6.08\ 10^{-2}$	$6.44\ 10^{-2}$	$8.62\ 10^{-2}$	$8.60\ 10^{-2}$
10.	$6.45\ 10^{-2}$	$6.47\ 10^{-2}$	$6.46\ 10^{-2}$	$6.55\ 10^{-2}$	$6.49\ 10^{-2}$	$6.49\ 10^{-2}$	$9.62\ 10^{-2}$	$9.91\ 10^{-2}$
12.	$6.30\ 10^{-2}$	$6.26\ 10^{-2}$	$6.26\ 10^{-2}$	$6.38\ 10^{-2}$	$6.30\ 10^{-2}$	$6.30\ 10^{-2}$	$9.35\ 10^{-2}$	$9.77\ 10^{-2}$
15.	$5.87\ 10^{-2}$	$5.94\ 10^{-2}$	$5.94\ 10^{-2}$	$6.12\ 10^{-2}$	$5.99\ 10^{-2}$	$5.99\ 10^{-2}$	$8.81\ 10^{-2}$	$9.42\ 10^{-2}$

Table II. Same as Table 1. except V =15. Note that in columns LB and LW at T=0.5 the rate could not be determined since the minimal value of the correlation function obtained is on the order of 10 which is much larger then the rate itself at this temperature.

T	Exact GR	Ref. 12b	LHA	HTL	LB	LW	C1	C2
0.	$8.48\ 10^{-22}$	$-6.9\ 10^{-14}$	$-6.9\ 10^{-14}$	–	–	–	–	–
.5	$4.24\ 10^{-13}$	$4.15\ 10^{-12}$	$3.96\ 10^{-13}$	$6.72\ 10^{-9}$	–	–	$-2.8\ 10^{-18}$	$-1.56\ 10^{-8}$
1.	$9.64\ 10^{-8}$	$-1.4\ 10^{-8}$	$1.43\ 10^{-7}$	$6.96\ 10^{-7}$	$8.25\ 10^{-8}$	$2.40\ 10^{-7}$	$3.09\ 10^{-13}$	$-2.53\ 10^{-9}$
2.	$8.98\ 10^{-5}$	$7.10\ 10^{-5}$	$9.68\ 10^{-5}$	$1.19\ 10^{-4}$	$8.75\ 10^{-5}$	$1.01\ 10^{-4}$	$1.52\ 10^{-7}$	$2.30\ 10^{-8}$
3.	$8.63\ 10^{-4}$	$8.23\ 10^{-4}$	$8.85\ 10^{-4}$	$9.39\ 10^{-4}$	$8.58\ 10^{-4}$	$8.94\ 10^{-4}$	$1.84\ 10^{-5}$	$8.89\ 10^{-7}$
5.	$4.88\ 10^{-3}$	$4.87\ 10^{-3}$	$4.91\ 10^{-3}$	$4.96\ 10^{-3}$	$4.87\ 10^{-3}$	$4.91\ 10^{-3}$	$8.73\ 10^{-4}$	$5.37\ 10^{-4}$
10.	$1.53\ 10^{-2}$	$1.55\ 10^{-2}$	$1.54\ 10^{-2}$	$1.53\ 10^{-2}$	$1.53\ 10^{-2}$	$1.53\ 10^{-2}$	$1.32\ 10^{-2}$	$1.06\ 10^{-2}$
12.	$1.78\ 10^{-2}$	$1.81\ 10^{-2}$	$1.81\ 10^{-2}$	$1.79\ 10^{-2}$	$1.79\ 10^{-2}$	$1.79\ 10^{-2}$	$1.96\ 10^{-2}$	$1.62\ 10^{-2}$
15.	$2.02\ 10^{-2}$	$2.08\ 10^{-2}$	$2.08\ 10^{-2}$	$2.04\ 10^{-2}$	$2.05\ 10^{-2}$	$2.05\ 10^{-2}$	$2.81\ 10^{-2}$	$2.43\ 10^{-2}$

Also, the methods based on Eqs. (5)-(6) and (7)-(8) become free of pathologies because the thermal averages of the exponential function in (5) and of the integrand in (8b) decay to zero at large times, leading to convergent integrals. Still, the correlation function C(t) calculated from the classical analog of Eq. (5) shows unphysical recurrences at long times, and the results in columns LB and LW of Tables 1 and 2 were obtained by truncating the integration in Eq. (1) before this happens.

Tables 1 and 2 summarize the results for the thermal rates obtained with the different approximate methods outlined above. The results are presented for several temperatures at two different values of the crossing energy, V_c=3.5 and V_c=15. The dimensionless value of the parameter α was taken α=6 as before.[13b] The following observations can be made:

(a) The result of Ref. 13b as well as those in columns LB, C1 and C2 of tables 1 and 2 were obtained using a classical canonical averaging over the initial nuclear states. Some improvement at low temperatures can be expected by replacing this by an average over the corresponding Wigner distribution for the initial harmonic surface,

$$\rho_W(x,p)=\frac{\tanh(\frac{1}{2}\beta\hbar\omega)}{\pi\hbar}\exp\left\{-\frac{1}{\hbar\omega}\tanh(\tfrac{1}{2}\beta\hbar\omega)\left(\frac{p^2}{m}+m\omega^2x^2\right)\right\} \quad (27)$$

In practice we found this does not improve the low temperatures results considerably.

(b) All the procedures tested, except the cumulant expansion method, perform well for high enough temperatures, typically for $T/\hbar\omega \geq 2$. For lower temperatures the local harmonic approximation is superior to the procedure of Ref. 13b.

(c) The calculation based on the semiclassical analog of Eq. (5) does surprisingly well, however it may become tedious for more complicated models, due to possible slow convergence.

(d) For the present model, the cumulant expansion method does significantly more poorly than the the other methods. The source of the problem can be seen by comparing (Fig. 2) the correlation functions, C(t), obtained in this approximation to the same function obtained in the LHA (which is practically exact in the present model). Two cumulant approximations are obtained by doing the classical evolution on the two potential surfaces. The correlation

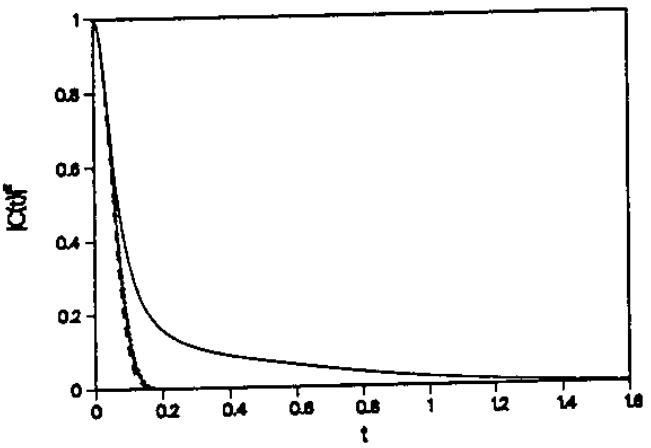

Fig. 2: The absolute square of the correlation function, Eq. (2), for the model of Fig. 1 at $T/\hbar\omega = 10$. The full line represents the result of the local harmonic approximation (essentially exact for this case). The other, almost overlapping lines, represent results from different versions of the cumulant approximation defined in the text (propagation on the harmonic or the linear surface; sampling with Wigner function or exact quantum mechanical sampling), which in the present case give very similar results.

functions obtained from these methods decay too fast, indicating the importance of the neglected higher cumulants. It should be emphasized that this method is expected to do better in higher dimensional situations, where the character of the local coordinates which dominate the transition may become more Gaussian.[12]

(e) For the model considered here the LHA is practically exact; the only remaining approximation in our procedure is the use of frozen Gaussians. In fact, thawed Gaussians can be used with almost equal ease. Indeed, when this is done the exact rate is obtained.

IIIb. Displaced harmonic oscillators In this model surfaces 1 and 2 are harmonic wells with equal frequencies, displaced both in position and energy. A review of the model is given in Ref 13b. The exact rate is given by Eq. (1) with

$$C(t)=\exp\left\{-i\Delta Et/\hbar+im\omega d^2\sin(\omega t)/2\hbar - \frac{m\omega d^2}{2\hbar}\coth(1/2\beta\hbar\omega)[1-\cos(\omega t)]\right\} \quad (28)$$

It is obvious that the LHA result (23) is exact for this model and the rate obtained from Eq. (25) will therefore be exact if full quantum propagation is used. Surprisingly, the exact rate is obtained also when the FGA scheme is used, although the FGA propagation is exact only in the special case where the Gaussian width

is chosen to be that of the exact ground state (coherent wave), $a=m\omega/\hbar$. This indicates that the errors associated with the FGA propagation on the two identical potential surfaces cancel out.

Consider now the results based on (5)-(6) and (7)-(8). Here the calculation can be done analytically. Applying the Wigner distribution for the thermal averaging of the semiclassical analog of the correlation function in Eq. (5) leads to

$$C(t) = \exp\left\{-i\Delta E t/\hbar + im\omega^2 d^2 t/2\hbar - \frac{m\omega d^2}{2\hbar}\coth(1/2\beta\hbar\omega)[1-\cos(\omega t)]\right\} \quad (29)$$

The same result is obtained from the cumulant expansion method, Eqs. (7)-(8), when classical nuclear dynamics and a Wigner distribution of initial states are used. Eq. (29) is a short time approximation to the exact correlation function (28). This approximation is known to yield reliable results only in the "strong coupling limit" when the two surfaces are strongly displaced from each other.

IV Summary and Conclusions

We have presented improved methods for calculating the golden rule expression for non-adiabatic transition rates from computer simulations. These methods are based on forming initial thermal wavepackets $e^{-\frac{1}{2}\beta H}|x\rangle$ by imaginary time propagation, following Hellsing et al,[22] and representing them as Gaussians. This can be accomplished in the high temperature limit (HTL) or in the local harmonic approximation (LHA). The real time evolution of these Gaussians then yields the correlation function C(t), Eq. (2), which in turn is used to calculate the rate, Eq. (1). In most cases it is sufficient to use the Frozen Gaussians approximation (FGA) for the real time evolution. In this case only classical trajectories are required. More sophisticated propagation techniques may be used.

The new procedures described in this work provide three major improvements over out previous method.[13] (1) The initial Gaussian width is now determined unambiguously by the procedure without additional assumptions. (2) The thermal averaging involves sampling in configuration space and not in phase space. (3) At low temperatures this sampling uses an improved probability function.

The implementation of this method for a many body system at low temperatures requires the use of the LHA in the normal mode representation at each initial configuration (Appendix B). Instantaneous normal mode analysis in molecular liquid simulation were recently shown to be feasible.[24] In this case the sampling of initial configuration involves a probability function defined in terms of an effective potential as described in Appendix B.

We have also tested the semiclassical approximation suggested by Lax[12] and recently applied by several workers.[17-19] The semiclassical analog of Eq. (5) (obtained by replacing the exponential in (5) by its classical counterpart) performed surprisingly well when the temperature is not too low. The second order cumulant approximation did not perform well in our one dimensional example, but is expected to do better in more realistic multidimensional situations in the high temperature limit.

Appendix A. An outline of the frozen Gaussian approximation (FGA)

The FGA[20] needs only classical information in order to propagate the initial Gaussian wavepacket (Eq. (4)). The initial conditions for the classical motion are x_0 and p_0 from which the position, x_t, and momentum, p_t, at time t are obtained by solving the classical equations of motion. The wavepacket at time t is given by

$$G(x,t) = \left(\frac{a}{\pi}\right)^{1/4} \exp\left(-\tfrac{1}{2}a(x-x_t)^2 + i\hbar p_t(x-x_t) + i\phi(t)/\hbar\right) \quad (A1)$$

with the phase ϕ given by

$$\phi(t) = \int_0^t dt' L(t') \quad (A2a)$$

$$L(t') = \frac{p_t^2}{m} - \langle G(t)|H|G(t)\rangle \quad (A2b)$$

Appendix B. The Local Harmonic Approximation in the multidimensional case.

In analogous manner to the 1-dimensional case, Eq. (17), we develop V(x) up to second order about the point of interest, x'

$$V(\mathbf{x}) = V(\mathbf{x}') + \sum_i \left.\frac{\partial V}{\partial x_i}\right|_{\mathbf{x}=\mathbf{x}'} (x_i - x'_i)$$

$$+\tfrac{1}{2}\sum_{i,j} \left.\frac{\partial^2 V}{\partial x_i \partial x_j}\right|_{\mathbf{x}=\mathbf{x}'} (x_i - x'_i)(x_j - x'_j)$$

$$= V(\mathbf{x}') + \sum_i \eta_i (x_i - x'_i) + \tfrac{1}{2}\sum_{i,j} k_{ij}(x_i - x'_i)(x_j - x'_j)$$

$$= V(\mathbf{x}') + \sum_i \eta_i \delta_i + \tfrac{1}{2}\sum_{i,j} \frac{k_{ij}}{\sqrt{m_i m_j}} X_i X_j \qquad \text{(B1)}$$

where

$$X_i = \sqrt{m_i}\,(x_i - x'_i - \delta_i) \qquad \text{(B2a)}$$

$$\delta_i = \frac{|\mathbf{K}_i|}{|\mathbf{K}|} \qquad \text{(B2b)}$$

$\mathbf{K}$ is a matrix whose elements are k_{ij}. $\mathbf{K}_i$ is the matrix $\mathbf{K}$, with the i-th column replaced by the vector η_i. Next, a transformation to normal mode $\mathbf{Q}$ of the harmonic potential (B1) is done using the appropriate orthogonal transformation matrix $\mathbf{D}$,

$$\mathbf{Q} = \mathbf{D}^{-1}\mathbf{X} \qquad \text{(B3)}$$

$\mathbf{X}$ is the vector of elements X_i. The Gaussian thermal wavepacket, Ψ (Eq. 11) is obtained in the form

$$\Psi_{\mathbf{x}'}(\mathbf{x}) = \prod_i \left\{\frac{m_i^2 \omega_i}{\pi\hbar \sinh(\beta\hbar\omega_i)}\right\}^{1/4} \times \exp\left\{\frac{\omega_i}{2\hbar}\tanh(1/2\beta\hbar\omega_i) Q_{0_i}^2\right\} \Psi_{\overline{Q}_i}(Q_i(\mathbf{x})) \qquad \text{(B4a)}$$

$$\Psi_{\overline{Q}_i}(Q_i) = \left\{\frac{\omega_i \coth(1/2\beta\hbar\omega_i)}{2\pi\hbar}\right\}^{1/4} \times \exp\left\{-\frac{\omega_i}{2\hbar}\coth(1/2\beta\hbar\omega_i)(Q_i - \overline{Q}_i)^2\right\} \qquad \text{(B4b)}$$

ω_i is the frequency of the i-th normal mode,

$$Q_{0_i}(Q_i) = -\sum_j D_{ji}\sqrt{m_j}\,\delta_j \qquad \text{and} \qquad \overline{Q}_i = Q_{0_i} / \cosh(\tfrac{1}{2}\beta\hbar\omega_i).$$

In these equations the normal modes Q_i are related to the original coordinates x_i by equations (B2) and (B3). Using the following definition

$$\Psi_{\overline{Q}} = \prod_i \Psi_{\overline{Q}_i}(Q_i) \qquad \text{(B5)}$$

the matrix element required for the calculation of the correlation function in Eq. (10) is given by

$$\left\langle \Psi_{\mathbf{x}'} \middle| F_{21} \middle| \Psi_{\mathbf{x}'} \right\rangle = \int d\mathbf{x} \Psi_{\mathbf{x}'}(\mathbf{x}) F_{21}(\mathbf{x}) \Psi_{\mathbf{x}'}(\mathbf{x}) = \prod_i \left\{\frac{m_i \omega_i}{\pi\hbar \sinh(\beta\hbar\omega_i)}\right\}^{1/2} \times \exp\left\{\frac{\omega_i}{\hbar}\tanh(1/2\beta\hbar\omega_i) Q_{0_i}^2\right\} \times \left\langle \Psi_{\overline{Q}} \middle| F_{21} \middle| \Psi_{\overline{Q}} \right\rangle_Q \qquad \text{(B6)}$$

with

$$\left\langle \Psi_{\overline{Q}} \middle| F_{21} \middle| \Psi_{\overline{Q}} \right\rangle = \int d\mathbf{Q} \Psi_{\overline{Q}}(\mathbf{Q}) F_{21}(\mathbf{x}(\mathbf{Q})) \Psi_{\overline{Q}}(\mathbf{Q}) \qquad \text{(B7)}$$

The correlation function, Eq. (10), is finally given by

$$C(t)=\frac{1}{Z_1}\int dx' \exp\{-\beta[V(x')+ \frac{1}{2}\sum_i \eta_i(x')\delta_i(x')]\}\langle\Psi_{x'}|F_{21}|\Psi_{x'}\rangle \quad \text{(B8)}$$

The thermal wave packet can now be propagated by using the FGA in the Q coordinates. This can be done by sampling the initial conditions in configuration space according to the probability function appearing in Eq. (B8). The propagation of the thermal wave packet can be performed in two ways: (a) The equations of motion are solved in the x coordinates and the solution transformed to the normal coordinates Q in order to obtain the time propagation of $\Psi_{\overline{Q}}(Q)$ (b) The Hamiltonians H_1 and H_2 are transformed to the normal coordinates and the equations of motion can be now be explicitly solved using the normal coordinates.

To summarize the procedure : A point x' is chosen according to the "effective potential" $V(x')+1/2\sum_i \eta_i(x')\delta_i(x')$. H_1 is expanded up to second order in the coordinates about the point x'. The quadratic Hamiltonian is diagonalized and the eigenvalues ω_i^2 and normal coordinates Q_i are obtained. A Gaussian wave packet, (B4), is located with the center at $\overline{Q}$. Two ways are available to propagate the initial wavepacket. Either transforming H_1 and H_2 to the normal coordinates and solving the equations of motion starting at $\overline{Q}$, or solving the equations of motion in the x coordinates starting at $x(\overline{Q})$ and transforming the resulting trajectory to the Q coordinates.

Finally note that the high temperature limit of the multidimensional correlation function, Eq. (B8), yields the HTL result, Eq. (16).

Acknowledgement

We thank Professors R. D. Coalson, H. Metiu and M. Ratner for very helpful discussions. This work was supported in part by the Israel National Science Foundation.

References

[1]See papers in *Time Dependent Methods for Quantum Dynamics*, Comp. Phys. Comm. **63**, (1991)
[2]R. Kosloff, J. Phys. Chem. **92** 2087 (1988)
[3]P. J. Rossky and J. Schnitker, J. Phys. Chem. **92**, 4277 (1988); T. H. Murphery and P. J. Rossky;J. Chem. Phys. **99**, 515 (1993); R. N. Barnett, U. Landman and A. Nitzan, J. Chem. Phys. **89**, 2242 (1989); **93**, 8187 (1990); R. N. Barnett, U. Landman, G. Rajagopal and A. Nitzan, Isr. J. Chem. **30**, 85 (1990); R. A. Kuwarski, J. S. Bader, D. Chandler, M. Sprik, M. L. Klein and R. W. Impey, J. Chem. Phys. **89**, 3248 (1989).
[4](a) S. Sawada and H. Metiu, J. Chem. Phys. **84**, 227 (1985) (b) M. Messina and R. D. Coalson, J. Chem. Phys. **92**, 5712 (1990); **95**, 5364 (1991)
[5]J. C. Tully, J. Chem. Phys. **93**, 1061 (1990).
[6]J. C. Tully and R. K. Preston, J. Chem. Phys. **55**, 562 (1971).
[7](a) B. Martire and R. G. Gilbert, Chem. Phys. **56**, 241 (1981); (b) D. P. Ali and W. H. Miller, J. Chem. Phys. **78**, 6640 (1983).
[8](a) N. Makri and W. H. Miller, J. Chem. Phys. **87**, 5781 (1987); (b). Z. Kotler, A. Nitzan and R. Kosloff, Chem. Phys. Lett. **153**, 483 (1988); (c) Z. Kotler, E. Neria and A. Nitzan, Comp. Phys. Comm. **63**, 243 (1991). (d) A. D. Hammerich, R. Kosloff and M. A. Ratner, Chem. Phys. Lett. **171**, 97 (1990). (e) H.-D. Meyer, U. Manthe and L. S. Cederbaum, Chem. Phys. Lett. **165**, 73 (1990); J. Chem. Phys. **97**, 3199 (1992); (f) R. Kosloff and A. D. Hammerich, Far. Disc. Chem. Soc. **91**, 239 (1991); (g) J. C. Martinez, J. R. Waldeck and R. D. Coalson, J. Chem. Phys. **96**, 3613 (1992).
[9]P. Pechukas, Phys. Rev. **181**, 166; 174 (1969).
[10](a) F. J. Webster, J. Schnitker, M. S. Friedrich, R. A. Friesner and P. J. Rossky, Phys. Rev. Lett. **66**, 3172 (1991); (b) F. J. Webster, P. J. Rossky and R. A. Friesner, Comp. Phys. Comm. **63**, 494 (1991).
[11](a) B. Space and D. F. Coker, J. Chem. Phys. **94**, 1976 (1991); (b) B. Space and D. F. Coker, J. Chem. Phys. **96**, 652 (1992).
[12]M. Lax, J. Chem. Phys. **20**, 1752 (1952)
[13](a) E. Neria, A. Nitzan, R. N. Barnett and U. Landman, Phys. Rev. Lett. **67**, 1011 (1991). (b) E. Neria and A. Nitzan, (J. Chem. Phys. **99**, 2343 (1993). (c) M. D. Todd, A. Nitzan and M. A. Ratner, J. Phys. Chem. **97**, 29 (1993).
[14](a) E. J. Heller, J. Chem. Phys. **68**, 2066 (1978); S. Y. Lee and E. J. Heller, J. Chem. Phys. **71**, 4777 (1979) (b) E. J. Heller and R. C. Brown, J. Chem. Phys. **79**, 3336 (1983). (c) J. R. Reimers, K. R. Wilson and E. J. Heller, J. Chem. Phys. **79**, 4749 (1983).
[15]P. Vilarreal, S. Miret-Artés, O. Roncero, G. Delgado-Barrio, J. A. Beswick, N. Halberstadt and R. D. Coalson, J. Chem. Phys. **94**, 4230 (1991).
[16]M.F. Herman, J.Chem.Phys. **87**, 4779; 4794 (1987).
[17](a) A. Warshel, J. Phys. Chem. **86**, 2218 (1982) (b) A. Warshel and J. K. Hwang, J. Chem. Phys **84**, 4938 (1986); (c) A. Warshel and W. W. Parson, Ann. Rev. Phys. Chem., **42**, 279 (1991) and references therein

[18](a) M. Sparpaglione and S. Mukamel, J. Phys. Chem. **91**, 3938 (1987); (b) M. Sparpaglione and S. Mukamel, J. Chem. Phys. **88**, 3263 (1988); (c). M. Sparpaglione and S. Mukamel, J. Chem. Phys. **88**, 4300 (1988); (d). Y. J. Yan and S. Mukamel, J. Chem. Phys. **88**, 5735 (1988). Other relevant papers by Mukamel and co-workers are cited in these references.
[19]D. Borgis and J.T. Hynes, J. Chem. Phys. **94**, 3619 (1991).
[20]E. J. Heller, J. Chem. Phys. **75**, 2923 (1981).
[21]E. J. Heller, J. Chem. Phys. **62**, 1544 (1975).
[22]B. Hellsing, S. Sawada and H. Metiu, Chem. Phys. Lett. **122**, 303 (1985).
[23]R. P. Feynman, *Statistical Mechanics*, (W. A. Benjamin, Reading Mass. 1972).
[24]M. Buchner, B. M. Ladanyi and R. M. Stratt, J. Chem. Phys. **97**, 8522 (1992).